Laminar Natural Convection in a High-Aspect-Ratio Inclined Rectangular Duct

D. Majumdar,* J. Y. Murthy,† and R. P. Roy‡
Arizona State University, Tempe, Arizona

Natural convection heat transfer in a high-aspect-ratio rectangular duct with one wall subjected to a uniform heat flux and the other wall insulated has been analyzed. A control-volume-based numerical technique has been used in the analysis. Calculations were mainly performed for the corresponding two-dimensional channel flow. Some three-dimensional duct flow computations were carried out in order to validate the channel flow approximation. Numerical results are reported for different combinations of mass flow rates and channel (duct) inclinations to the horizontal. Local Nusselt numbers as well as velocity and temperature distributions are presented.

Nomenclature

b = spacing between the top and bottom walls of duct or channel
c_f = skin friction coefficient, defined by Eq. (14)
c_p = specific heat of fluid
g = acceleration due to gravity
Gr = channel Grashof number, $=g\beta\,(qb/k)\,b^3/\nu^2$
Gr^* = modified Grashof number, $=Grb/\ell$
h = convective heat transfer coefficient
k = thermal coductivity of fluid
ℓ = channel length
M_{in} = inlet mass flow rate parameter, $=w_{in}b/\nu Gr$
Nu_z = local Nusselt number, $=h(z)b/k$
p = fluid pressure
p' = pressure defect, $=p-p_\infty$
$\bar{p}$ = cross-sectional mean pressure at any elevation
p_∞ = local hydrostatic fluid pressure
$\overline{p'}$ = pressure defect based on $\overline{p'}$, $=\bar{p}-p_\infty$
Pr = Prandtl number, $=\mu c_p/k$
q = heat flux
T = fluid temperature
T_B = bulk temperature defined by Eq. (13)
T_W = heated wall temperature
T_∞ = temperature of the fluid at channel entrance
u,v,w = fluid velocity in the x, y, and z directions, respectively
w_{in} = fluid velocity at channel entrance
x = coordinate along duct width
y, z = rectangular coordinate system, Fig. 1
β = volumetric coefficient of thermal expansion
Θ = dimensionless temperature, $=(T-T_\infty)/(qb/k)$
θ = angle of inclination to horizontal
μ = dynamic viscosity of fluid
ν = kinematic viscosity of fluid
ρ = density of fluid
τ = wall shear stress

Subscript

h = heated wall

Received July 2, 1988; revision received Sept. 13, 1988.

*Graduate Student, Department of Mechanical and Aerospace Engineering.
†Assistant Professor, Department of Mechanical and Aerospace Engineering.
‡Professor, Department of Mechanical and Aerospace Engineering.

Introduction

NATURAL convection arises from the buoyancy forces induced by density differences in a fluid. Since this mechanism plays an important role in heat transfer in a large variety of internal and external flows, it has received a great deal of attention in the research community. The vertical flat plate is the limiting case of the vertical two-dimensional channel and has undergone detailed investigation due to its simple geometry.[1,2] The inclined flat plate has also received a considerable amount of attention.[3-6] The early channel flow literature is due to Elenbaas,[7] who performed experiments with a variable geometry isothermal channel in air. Steady laminar free convection between vertical parallel plates was first analyzed by Bodoia and Osterle,[8] using a finite-difference technique. Engel and Mueller[9] used an integral technique to investigate the development of natural convection in vertical channels of finite length. Aung et al.[10] performed a combined numerical and experimental investigation of laminar free convection in air in a vertical channel, where the walls were either individually subjected to uniform heat flux or maintained at constant temperature. Wirtz and Stutzman[11] presented experimental data for natural convection in air between vertical parallel plates subjected to uniform and symmetric heat fluxes.

In the case of natural convection, to the present authors' knowledge, all published results have been either for vertical and inclined flat plates or for vertical channels. The influence of natural convection on flows in inclined channels has not been fully investigated.

The purpose of this study is to examine the internal flow induced in an inclined rectangular duct with differentially heated side walls. The heated wall, being inclined with respect to gravity, imposes a buoyancy component along the duct axis, thus inducing an axial flow. The flow entrained is dependent, among other parameters, on the length of the duct. The most important feature of this flow is that the pumping action is entirely due to wall heating—there is no externally imposed pressure gradient. If the width of the duct is much greater than its wall spacing (a high aspect ratio duct), it should be possible to approximate the three-dimensional flow in the duct well by a two-dimensional channel flow (Fig. 1). The present investigation analyzes both flow situations and concludes that the use of the two-dimensional flow approximation is justified in the case of a high-aspect-ratio duct. The control-volume-based numerical technique described in Ref. 12 is used in conjunction with a marching procedure in the axial direction.

Analysis

Consider steady laminar flow in a rectangular channel oriented at any angle θ to the horizontal (Fig. 1). The length of

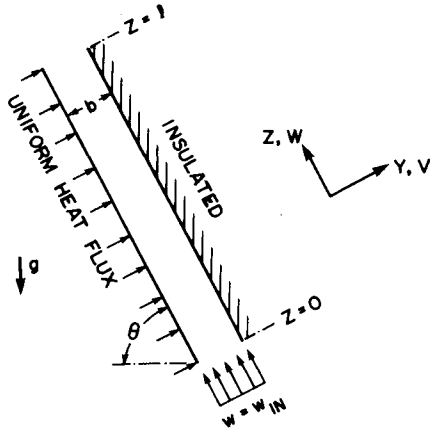

Fig. 1 Channel geometry.

the channel is ℓ, and the channel spacing (or height) is b. The bottom wall of the channel is subjected to a uniform heat flux and the top wall is insulated. When duct flow is considered, the two side walls are also insulated. As a result of heat transfer, the fluid near the hot wall rises and induces the flow. The pressure in the channel at any cross section is, in general, lower than that outside the same axial location. The pressures at the inlet and outlet are, however, each equal to that outside. The computational scheme exploits this feature to calculate the channel length as a function of the inlet mass flow rate.

For internal flows, the parabolic flow model is frequently used. This model is appropriate if the governing differential equations (the Navier-Stokes equations) can be adequately approximated as parabolic in one coordinate. This is possible if 1) there exists a single predominant flow direction along which no reversal of flow takes place, 2) the diffusion of transported quantities (energy and momentum, for example) is negligible in the streamwise direction, and 3) the downstream pressure field has little influence on the upstream flow. The present computations employ the parabolic flow model.

The difference between the pressure p at any axial level within the channel and the hydrostatic pressure p_∞ at the same elevation outside is referred to as the pressure defect p'. The hydrostatic pressure decreases with elevation according to the relations

$$\frac{\partial p_\infty}{\partial y} = -\rho g \cos\theta \qquad \frac{\partial p_\infty}{\partial z} = -\rho g \sin\theta \tag{1}$$

The pressure and the gravity terms in the y-momentum equation may now be combined as follows:

$$-\frac{\partial p}{\partial y} - \rho g \cos\theta \Rightarrow -\frac{\partial p'}{\partial y} - g \cos\theta(\rho - \rho_\infty) \tag{2}$$

The density difference, $\rho - \rho_\infty$, may be approximated by a simplified equation of state:

$$\rho = \rho_\infty[1 - \beta(T - T_\infty)] \tag{3}$$

Therefore,

$$-\frac{\partial p}{\partial y} - \rho g \cos\theta \Rightarrow -\frac{\partial p'}{\partial y} + \rho_\infty g\beta \cos\theta(T - T_\infty) \tag{4}$$

Similarly, for the z-momentum equation,

$$-\frac{\partial p}{\partial z} - \rho g \sin\theta \Rightarrow -\frac{d\bar{p}}{dz} - \rho g \sin\theta \Rightarrow -\frac{d\bar{p}'}{dz} + \rho_\infty \beta g \sin\theta(T - T_\infty) \tag{5}$$

Here, dp/dz has been substituted for $\partial p/\partial z$ in the z-momentum equation in conformity with the parabolic flow model practice.

The differential equations describing the conservation of mass, momentum, and energy can be conveniently expressed in dimensionless form by the use of the following variables:

$$Y = \frac{y}{b}, \quad Z = \frac{z}{bGr}, \quad V = \frac{vb}{\nu}, \quad W = \frac{wb}{\nu Gr}$$

$$\Theta = \frac{T - T_\infty}{qb/k}, \quad P' = \frac{p'b^2}{\rho\nu^2}, \quad \bar{P}' = \frac{\bar{p}'b^2}{\rho\nu^2 Gr^2} \tag{6}$$

The dimensionless parabolized equations are

Continuity:

$$\frac{\partial V}{\partial Y} + \frac{\partial W}{\partial Z} = 0 \tag{7}$$

y momentum:

$$V\frac{\partial V}{\partial Y} + W\frac{\partial V}{\partial Z} = -\frac{\partial P'}{\partial Y} + \frac{\partial^2 V}{\partial Y^2} + Gr \cos\theta\Theta \tag{8}$$

z momentum:

$$V\frac{\partial W}{\partial Y} + W\frac{\partial W}{\partial Z} = -\frac{d\bar{P}'}{dZ} + \frac{\partial^2 W}{\partial Y^2} + \sin\theta\Theta \tag{9}$$

Thermal energy:

$$V\frac{\partial \Theta}{\partial Y} + W\frac{\partial \Theta}{\partial Z} = \frac{1}{Pr}\frac{\partial^2 \Theta}{\partial Y^2} \tag{10}$$

The dimensionless boundary conditions are

Inflow conditions:

$$V = 0, \quad W = \frac{w_{in}b}{\nu Gr} = M_{in}, \quad \Theta = 0 \tag{11}$$

Wall conditions:

$$@Y = 0, \quad \frac{\partial \Theta}{\partial Y} = -1 \quad @Y = 1, \quad \frac{\partial \Theta}{\partial Y} = 0 \tag{12}$$

For the duct flow, an additional equation (the momentum equation in the direction x perpendicular to the y-z plane in Fig. 1) will be solved, along with the appropriate boundary conditions.

The parabolized governing equations, [Eqs. (7-10)], are quasi-two-dimensional in nature in the sense that they turn a completely elliptic two-dimensional problem into one that can be solved by a series of one-dimensional elliptic calculations. Since any station in the flow requires information only upstream of that station, only such information need be stored. The procedure involves a "marching solution" in which the parabolized equations are solved over a cross-stream plane of interest and then a forward step is taken. The procedure is repeated until the channel exit is reached.

The mass flow entrained by the channel is proportional, in part, to the length of the channel. Thus, the inlet mass flow rate M_{in} is not an independent variable, but is coupled to the channel length. The parabolization of the governing equations allows this dependence to be accounted for in a very convenient way. The inlet mass flow rate is considered to be independently specified, as in forced flow. Then, with the known inlet condition, solution is obtained by stepping from one cross-stream plane to the next until a plane is encountered where the pressure defect $\bar{P}'$ is zero. This plane is the exit plane of the channel. Thus, the calculation procedure, in effect, computes the length of the channel compatible with the prescribed inlet mass flow rate.

Table 1 Computed $\ell/(bGr)$ values for various mass flow rates and angles of inclination to horizontal

Mass flow rate, M_{in}	Angle of inclination to horizontal			
	$\theta = 45$ deg, $\times 10^{-4}$	$\theta = 60$ deg, $\times 10^{-4}$	$\theta = 75$ deg, $\times 10^{-4}$	$\theta = 90$ deg, $\times 10^{-4}$
0.0008	0.63	0.58	0.56	0.54
0.0025	3.3	3.0	2.9	2.7
0.075	1917	1725	1624	1325

The governing differential equations are numerically solved employing a modified version of the SIMPLER algorithm developed by Patankar.[12] A fully implicit scheme is employed in discretizing the z-direction gradients. The axial pressure gradient is calculated by the method proposed by Raithby and Schneider.[13] A nonuniform grid is used to resolve the wall boundary layers. For the channel, 28 grid points are used in the y direction, with about 125 steps in the axial direction. This provides an accuracy of about 0.1% in the average Nusselt number, compared to runs on even finer grids. The grid employed in the case of the duct is a 50×28 grid (50 in the x direction and 28 in the y direction) in the cross-sectional plane, with about 125 axial steps. The parameters for the various cases studied are listed in Table 1. The Prandtl number is chosen to be 0.7 (air). The Grashof number is so chosen as to reflect an appropriate combination of air properties, wall heat flux, and channel spacing. It will be shown later that the Grashof number does not influence the axial velocity and temperature fields at all. For the duct flow calculations, the aspect ratio (ratio of the width of the duct to its height) is fixed at 5:1.

Results and Discussion

The most important result is the relationship between the inlet mass flow rate and the length of the channel (or duct) required to produce this flow rate. These results are presented in a nondimensional form in Table 1. It can be seen that for a particular angle of channel inclination, higher mass flow rates are associated with higher $\ell/(bGr)$ values. A greater input of energy is required to pump the larger mass flow rate; consequently, the greater length. As the angle of inclination to horizontal becomes smaller, the component of gravity in the axial direction decreases and, consequently, a greater length is required to pump the same mass flow rate at the same heat flux. The computed axial velocity and temperature profiles for the vertical ($\theta = 90$ deg) channel are indicated in Fig. 2 for $M_{in} = 0.0025$. The heated wall corresponds to $y/b = 0$ and the insulated wall to $y/b = 1$. The profiles agree well with the results presented by Aung et al.[10]

Figure 3 shows the development of the axial velocity profile with distance along the channel. The temperature of the heated wall increases with the axial distance, thereby increasing the influence of buoyancy locally; consequently, the maximum velocity location shifts toward the heated wall.

The temperatures of both the heated wall and the fluid increase in the axial direction. Figure 4 shows the development of the quantity $T - T_B/T_W - T_B$ along the axial direction in the channel. The bulk temperature T_B is defined by

$$T_B = \int wT \, dy / \int w \, dy \qquad (13)$$

The profiles at $z = 0.58$, 0.90, and 0.99 indicate that flow is very nearly fully developed at the channel exit.

Figure 5 depicts a typical profile of the cross-stream velocity v. The fluid starts at the inlet with a uniform axial velocity, but because of wall friction the flow near the walls is immediately decelerated; so, the fluid flows away from both of the walls initially. However, quite soon (for example, $z/\ell = 0.1$ or even less in some situations), as one proceeds along the channel, wall heating causes the fluid across the entire wall spacing to flow toward the hot wall to compensate for the fluid acceleration in the axial direction.

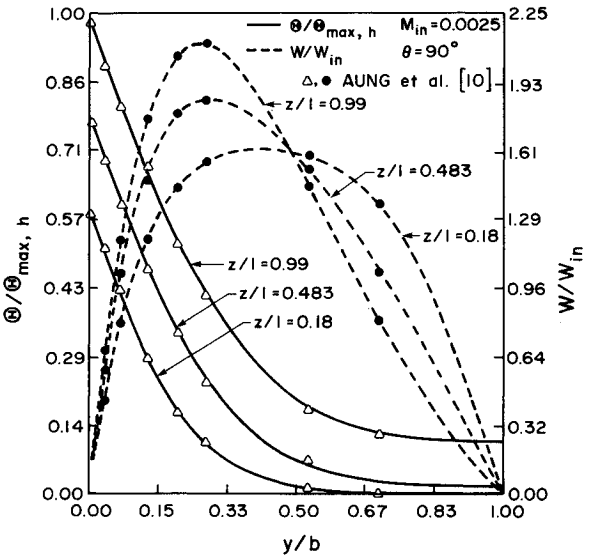

Fig. 2 Development of axial velocity and temperature profiles in the vertical channel (for $M_{in} = 0.0025$).

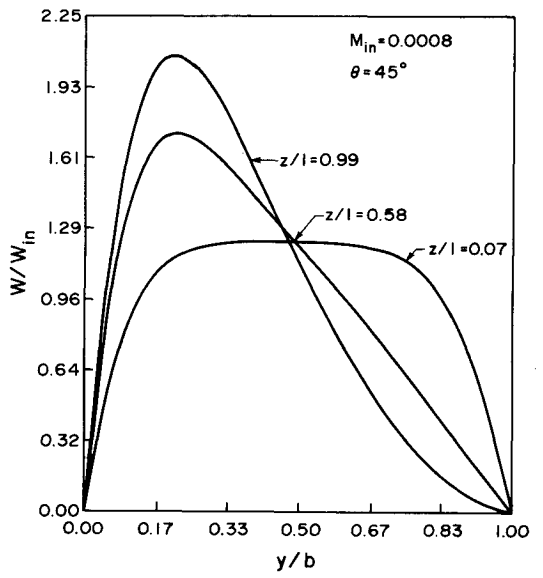

Fig. 3 Development of axial velocity profile (for $M_{in} = 0.0008$ and $\theta = 45$ deg).

Figure 6 compares the axial velocity and temperature profiles very near the channel exit for different angles of inclination. Though the general shapes of the profiles do not change very much with change in the inclination angle, the maximum axial velocity near the heated wall predictably decreases as the channel is tilted away from the vertical position. This effect also explains the behavior observed in Fig. 7, where the wall temperature is seen to increase with the tilt from the vertical.

If the inlet mass flow rate is increased while keeping the channel inclination the same, the buoyancy force decreases at a particular axial location due to the decrease of the temperture differential, causing the peak in the axial velocity near the heated wall to decrease as well as shift away from the wall.

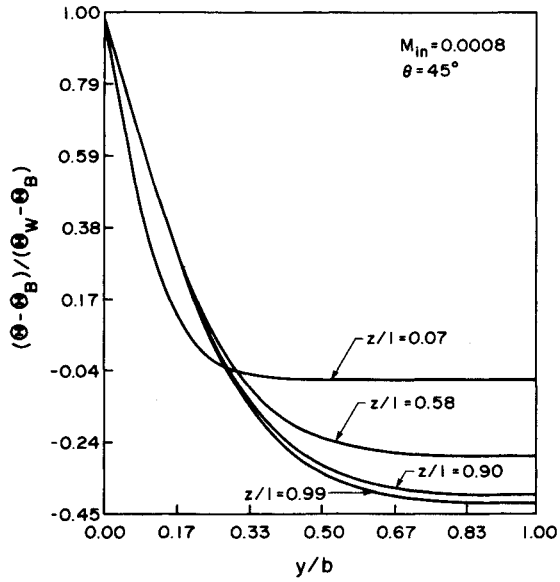

Fig. 4 Development of $T-T_B/T_W-T_B$ in the axial direction (for $M_{in}=0.0008$ and $\theta=45$ deg).

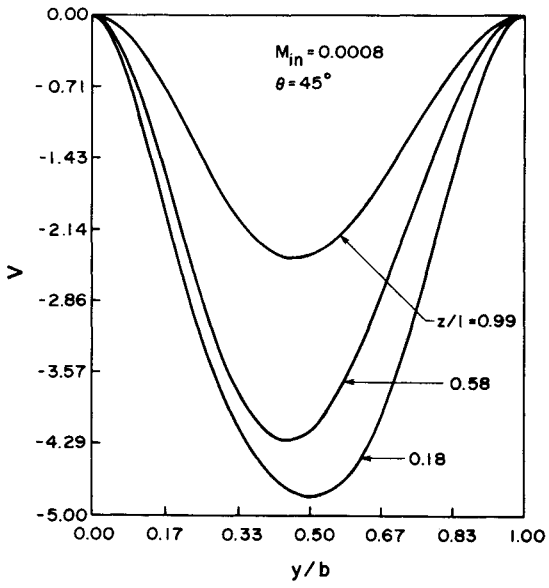

Fig. 5 Development of cross-stream velocity in the axial direction (for $M_{in}=0.0008$ and $\theta=45$ deg).

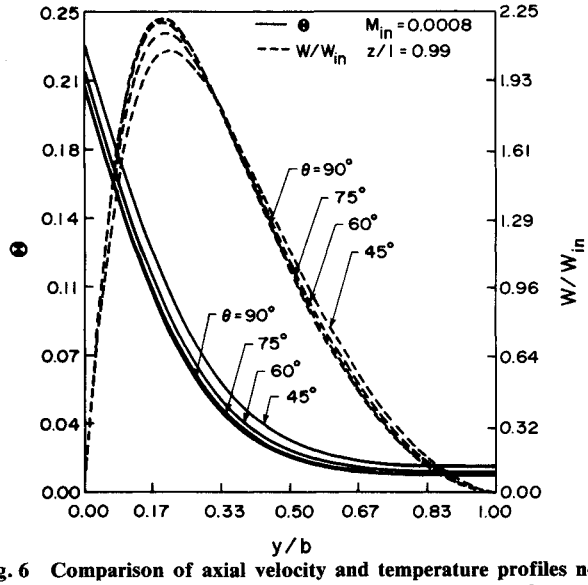

Fig. 6 Comparison of axial velocity and temperature profiles near channel exit for different angles of inclination to horizontal.

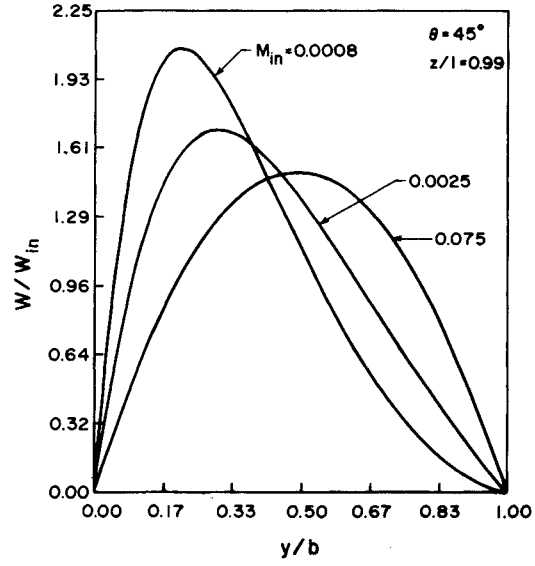

Fig. 7 Comparison of heated wall temperature variation in the axial direction for two different angles of inclination and mass flow rates.

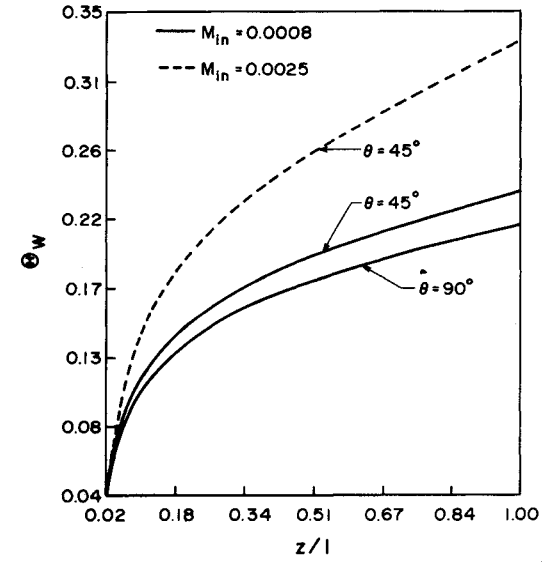

Fig. 8 Comparison of axial velocity profiles near channel exit for different values of mass flow rate.

This is depicted in Fig. 8, where the axial velocity profiles for three values of the mass flow rate have been compared at a location very near the channel exit.

The heated wall temperature is seen to increase at a faster rate at a higher mass flow rate. Recall that for $M_{in}=0.0025$, the axial velocity near the heated wall at any streamwise location is less than that for the case of $M_{in}=0.0008$. Therefore, less heat is convected away by the fluid near the wall as the mass flow rate increases; hence, the faster the increase in wall temperature at higher mass flow rate.

Figure 9 shows the variation of the shear stress at the heated wall along the channel. A skin friction coefficient is defined as

$$C_{fz}=\frac{\tau}{\frac{1}{2}\rho w_{in}^2}=\frac{\mu\dfrac{\partial w}{\partial y}\Big|y=0}{\frac{1}{2}\rho w_{in}^2}=\frac{2}{GrW_{in}^2}\frac{\partial W}{\partial Y}\Big|Y=0 \qquad (14)$$

and, therefore,

$$C_{fz}^{*}Gr=\frac{2}{W_{in}^2}\frac{\partial W}{\partial Y}\Big|Y=0 \qquad (15)$$

As has been noted earlier, Gr is not a parameter in so far as the velocity and temperature fields of this problem are con-

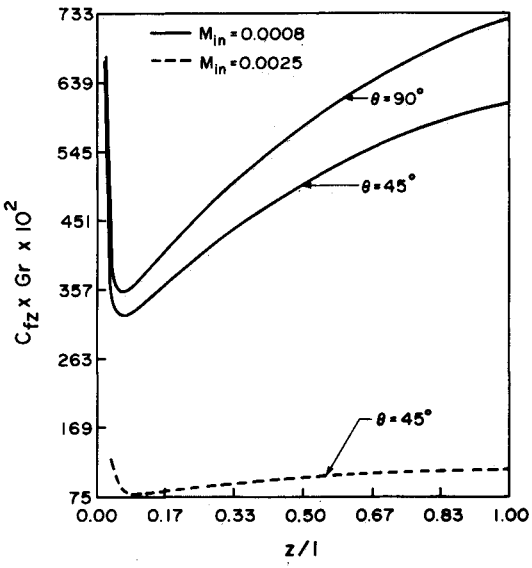

Fig. 9 Comparison of axial variation of shear stress at heated wall for two different angles of inclination and mass flow rates.

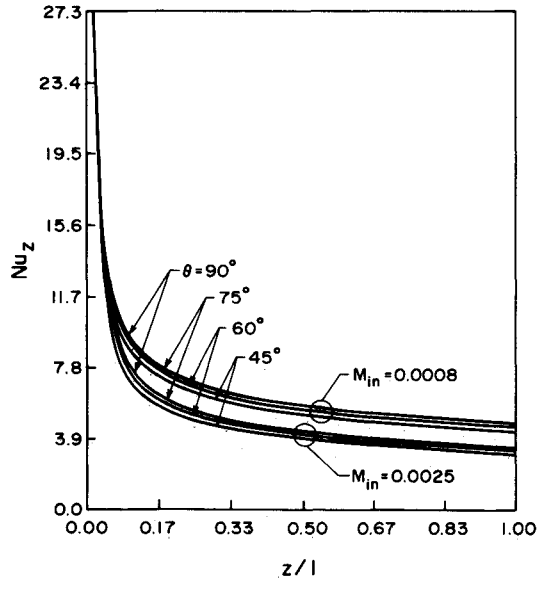

Fig. 10 Comparison of local Nusselt number variation in the axial direction for different angles of inclination at two different mass flow rates.

cerned, although it does appear in the dimensionless equations. A change in Gr merely changes the cross-stream pressure in the parabolic formulation [via Eq. (8)].

$C_{fz}^* Gr$ has been plotted in Fig. 9 vs the nondimensional axial distance. It can be seen that initially the value of the shear stress decreases, reaches a minimum, and then increases. This is because the gradient of the axial velocity at the heated wall decreases initially as a result of boundary-layer growth. However, the buoyancy forces soon begin to dominate and help accelerate the fluid in the axial direction. Consequently, the velocity gradient, and, therefore, the shear stress increase. For a given mass flow rate, the increase in the wall shear stress after the minima is more pronounced for the vertical channel than for the channel inclined at 45 deg. For the vertical case, the axial velocity near the heated wall is significantly larger than that for the inclined case, as is the velocity gradient at the heated wall. Consequently, the increase in $C_{fz}^* Gr$ (i.e., the shear stress) is more. One can also see from Fig. 9 that, for a given channel inclination, the increase of the wall shear stress after the minima is more pronounced for the lower mass flow rate situation. Since the axial velocity near the hot wall is significantly larger for the lower mass flow rate case, the axial velocity gradient at the wall is also much higher. Hence, a faster increase in the shear stress.

A comparison of the variation of the local Nusselt number along the channel for different angles of inclination and two values of mass flow rate is shown in Fig. 10. The local Nusselt number is defined as

$$Nu_z = \frac{h(z)b}{k} = \frac{q}{(T_W - T\infty)} \frac{b}{k} = \frac{1}{\Theta_W(z)} \tag{16}$$

As a general trend, the local Nusselt number decreases monotonically from the inlet to the exit of the channel. For a given mass flow rate, the Nusselt number decreases as the channel is tilted away from the vertical position. This is again due to the decreased axial velocity at the hot wall. At a particular angle of inclination to horizontal, the local Nusselt number decreases at a faster rate, at least near the entrance, as the mass flow rate is increased. This can be explained by the behavior of the heated wall temperature shown in Fig. 8, where a higher mass flow rate causes a faster increase in wall temperature.

Extensive computations for three-dimensional duct flow were performed for an aspect ratio of 5:1. For all of the cases considered, the results for the duct were essentially identical to the corresponding results for the channel. Calculations show that the order of magnitude of the cross-stream velocity in the x direction, u, in the duct is very small, being a factor of about 1000 lower than the axial velocity component w, and a factor of about 10 lower than the cross-stream velocity in the y direction v. Calculations also indicate that the difference between a typical duct flow result and channel flow result [e.g., the nondimensional channel length, $\ell/(bGr)$] is within half a percent. This, therefore, validates the channel flow approximation, i.e., for fairly large aspect ratios (for example, 5:1), the flow is almost one-dimensional in the cross-sectional plane. The u-momentum equation need not even be solved then.

Conclusions

Steady laminar natural convection heat transfer in an inclined rectangular duct and channel with differentially heated walls has been studied numerically. It has been found that for an aspect ratio of 5:1, the three-dimensional duct flow can be approximated well by two-dimensional flow in a channel. As the channel (or duct) is tilted away from the vertical position, the length required to sustain a given value of mass flow rate increases. Also, a longer channel induces a higher mass flow rate for a given angle of inclination to horizontal. At a given mass flow rate, as the channel (or duct) inclination to horizontal is increased, the axial velocity near the heated wall increases, the rate of increase of wall temperature decreases, the local Nusselt number decreases, and the increase of the wall shear stress along the channel after attaining the minimum is faster. If the mass flow rate is increased, keeping the angle of inclination at the same value, the peak in the axial velocity decreases and is shifted away from the heated wall, the wall temperature increases, the local Nusselt number decreases, and the increase of the wall shear stress after the minimum is slower.

The parabolic computation procedure is suitable as long as there is no reversed flow. In the present geometry, however, there exists possibility of flow reversal. For a particular inclination angle, if one decreases the channel length (which, in turn, decreases the mass flow rate induced) the natural convection process becomes more dominant and a larger fraction of the fluid flows near the heated wall. So, a situation may arise when the flow must undergo reversal near the cooler wall (in our case, the adiabatic wall) to maintain mass conservation. By the same token, for a particular mass flow rate, if the angle of inclination to horizontal is increased, the flow reversal is expected to occur much earlier along the channel. If one looks

closely at the axial velocity profiles near the channel exit in Figs. 3 and 6, it will be found that the velocity gradient at the adiabatic wall is extremely small, which gives rise to the suspicion that the flow may separate near the adiabatic wall for a sufficiently low value of mass flow rate at a given angle of inclination or as the vertical orientation is approached at a fixed mass flow rate. If flow reversal takes place, the present computational procedure can no longer be used and elliptic calculations with suitable outflow conditions must be employed.

References

[1]Ostrach, S., "An Analysis of Laminar Free Convection Flow and Heat Transfer about a Flat Plate Parallel to the Direction of the Generating Body Force," NACA Rept. 1111, 1953.

[2]Sparrow, E. M. and Gregg, J. L., "Laminar Free Convection From a Vertical Plate with Uniform Surface Heat Flux," *Transactions of the ASME,* Vol. 78, 1956, pp. 435–440.

[3]Rich, B. R., "An Investigation of Heat Transfer From an Inclined Flat Plate in Free Convection," *Transactions of the ASME*, Vol. 75, 1953, pp. 489–499.

[4]Kierkus, W. T., "An Analysis of Laminar Free Convection Flow and Heat Transfer about an Inclined Isothermal Plate," *International Journal of Heat and Mass Transfer*, Vol. 11, No. 2, 1968, pp. 241–253.

[5]Vliet, G. C., "Natural Convection Local Heat Transfer on Constant Heat Flux Inclined Surface," *Journal of Heat Transfer*, Vol. 91, 1969, pp. 511–515.

[6]Hassan, K. E. and Mohamed, S. A., "Natural Convection from Isothermal Flat Surfaces," *International Journal of Heat and Mass Transfer*, Vol. 13, 1970, pp. 1873–1886.

[7]Elenbaas, W., "Heat Dissipation of Parallel Plates by Free Convection," *Physica*, Vol. 9, 1942, pp. 1–28.

[8]Bodoia, J. R. and Osterle, J. F., "The Development of Free Convection Between Heated Vertical Plates," *Journal of Heat Transfer*, Vol. 84, 1962, pp. 40–44.

[9]Engel, R. K. and Mueller, W. K., "An Analytical Investigation of Natural Convection in Vertical Channels," ASME Paper 67-HT-16, 1967.

[10]Aung, W., Fletcher, L. S., and Sernas, V., "Developing Laminar Free Convection Between Vertical Flat Plates with Asymmetric Heating," *International Journal of Heat and Mass Transfer*, Vol. 15, 1972, pp. 2293–2308.

[11]Wirtz, R. A. and Stutzman, R. J., "Experiments on Free Convection Between Vertical Plates with Symmetric Heating," *Journal of Heat Transfer*, Vol. 104, 1982, pp. 501–507.

[12]Patankar, S. V., *Numerical Heat Transfer and Fluid Flow*, McGraw-Hill, New York, 1980.

[13]Raithby, G. D. and Schneider, G. E., "Numerical Solution of Problems in Incompressible Fluid Flow: Treatment of the Velocity Pressure Coupling," *Numerical Heat Transfer*, Vol. 2, 1979, pp. 417–440.